Advanced Materials Research Vol. 223 (2011) pp 514-522
Online available since 2011/Apr/19 at www.scientific.net

doi:10.4028/www.scientific.net/AMR.223.514

Modulation-Assisted Machining: A New Paradigm in Material Removal Processes

J.B. Mann[1,a], Y. Guo[2,b], C. Saldana[2,c], H. Yeung[2,d], W.D. Compton[2,e] and S. Chandrasekar[2,f]

[1]M4 Sciences LLC, 1201 Cumberland Ave, Suite A, West Lafayette, IN 47906, USA

[2]Center for Materials Processing and Tribology, School of Industrial Engineering
Purdue University, West Lafayette, IN 47907, USA

[a]jbmann@purdue.edu, [b]guo24@purdue.edu, [c]csaldana@purdue.edu, [d]hyeung@purdue.edu,
[e]dcompton@purdue.edu, [f]chandy@ecn.purdue.edu

Keywords: machining, modulation, chip, texture

Abstract. Modulation Assisted Machining (MAM), based on controlled superimposition of low-frequency modulation to conventional machining, effects discrete chip formation and disrupts the severe contact condition at the tool-chip interface. The underlying theory of discrete chip formation and its implications are briefly described and illustrated. Benefits such as improved chip management and lubrication, reduction of tool wear, enhanced material removal, particulate manufacturing and surface texturing are highlighted using case studies. MAM represents a new paradigm for machining in that it deliberately employs 'good vibrations' to enhance machining performance and capability.

Introduction

The mechanics of machining processes is unique in many respects. The formation of a continuous chip is an intrinsic characteristic of machining of ductile metals and alloys. However, continuous chips raise challenges associated with chip evacuation, interference with tooling, and lubrication of the tool-chip contact [1], and adversely impact machining performance. For example, in deep-drilling processes, the drilling performance, e.g., removal rate, tool wear, is often determined by the rate at which the continuous chips can be evacuated from inside the drilling zone which lies deep inside a hole. Indeed, application of fluid at high-pressure and flow-rate, so typical of many machining systems, is to break continuous chips into smaller, more easily manageable fragments and evacuate them from the machining zone. The tool-chip interface in continuous chip formation also represents an extreme tribological condition, characterized by high loads and elevated temperatures [1-4]. Consequently, fluid action is typically confined to the very edges of the contact [1, 3, 5-6]. The large strains typical of chip formation are also in part determined by the severity of the tool-chip contact condition [1]. Thus, if material removal with ductile alloys can be effected by 'discrete chip formation' and the severity of the tool-chip contact can be alleviated with enhanced fluid action, then the performance of machining processes (e.g., chip management, tool wear, fluid usage) could be enhanced. Machining with a controlled low-frequency modulation (< 1000 Hz) in the direction of feed – Modulation-Assisted Machining (MAM) – is shown to have achieve these in a controlled manner with attendant benefits to machining performance. Furthermore, MAM can be incorporated in industrial machining systems with minimal equipment modifications.

Background

Studies of application of controlled vibration to machining processes date back at least to the 1950s, especially discussion of consequences of 'chatter vibration' on chip formation [7, 8]. Findley [9], for example, also gives detailed consideration of modes of vibration to machining and some of

its consequences for chip formation. However, the underlying scientific details pertaining to the mechanics of chip formation receive less than adequate consideration. The major work on controlled vibration, though mainly of the ultrasonic kind, to 'assist' machining processes appears to have emerged from studies of Kumabe [10]. The modulation can be classified into a) modulation in the direction of cutting velocity – velocity-modulation and b) modulation in the direction of tool-feed or undeformed chip thickness – feed-modulation (Fig. 1).

Velocity-modulation. Consider machining with sinusoidal velocity-modulation. The cutting velocity varies during each cycle of modulation. In particular, the direction of instantaneous velocity is reversed and the tool-chip contact completely disrupted, during each modulation cycle, when the superimposed modulation velocity exceeds the mean (steady) cutting velocity; that is when $\omega A > V$, where ω is the angular modulation frequency and 2A is the peak-to-peak amplitude [11, 12]. While the velocity-modulation is effective at disrupting the tool-chip contact, enhancing fluid action and, potentially, lowering the contact temperature [11, 13], this approach has limitations. The disruption condition, $\omega A > V$ is difficult to realize in practice even at ultrasonic frequencies, except at the very low end of industrial machining speeds ($V < 0.5$ m/s), due to dynamic system level constraints [10, 14, 15]. This type of modulation does not result in discrete chips since the undeformed chip thickness is constant throughout the cutting. Also it is difficult to effect in processes such as drilling and boring, since the superimposed modulation would have to be rotary [15].

Geometry and Mechanics of MAM

A sinusoidal modulation, $A\sin(2\pi f_m t)$, may be superimposed in a direction parallel to the undeformed chip thickness. This is the configuration of interest to the present study - MAM. In MAM, the instantaneous undeformed chip thickness varies with time (t) as $h(t) = h_o + A\sin(2\pi f_m t)$, where h_o is the undeformed chip thickness in the absence of the modulation. If A is sufficiently large, then h(t) becomes less than or equal to zero during each cycle of modulation, resulting in 'discrete chips', these being produced at the rate of f_m per second. The tool-chip contact is then also disrupted f_m times per second [15, 16]. The critical value of the modulation amplitude (A) needed to realize discrete chip formation can be estimated for general machining configurations based on consideration of tool motion. Consider cylindrical turning, where a workpiece of diameter, d, is rotating at a frequency, f_w, and material is removed by feeding the tool at a rate of h_o per revolution. The critical amplitude, in non-dimensional form, is given by $A/h_o = 1 / [2\sin(\varphi/2)]$, where $\varphi = 2\pi (f_m/f_w - \text{INT}[f_m/f_w])$ $(0 \le \varphi < 2\pi)$ and 'INT[ ]' denotes the integer part of the value.

Fig. 1a shows this dependence of A/h_o on φ in graphical form. Since φ depends only on f_m/f_w, A/h_o can also be plotted as a function of f_m/f_w as in Fig. 1b; in this latter framework, the single curve

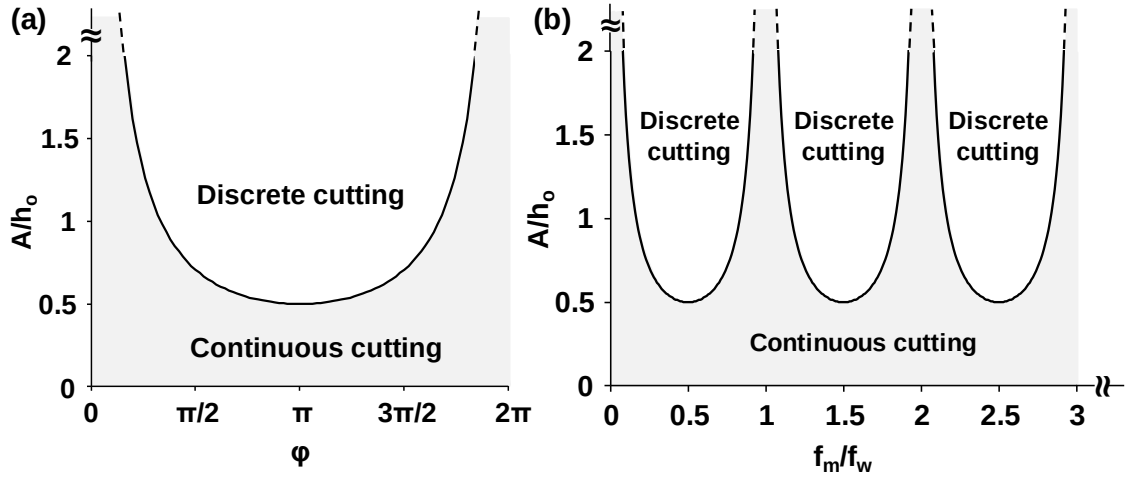

Figure 1 Cutting regimes of MAM in (a) φ – A/h_o space and (b) f_m/f_w – A/h_o space. The transition from continuous cutting to discrete cutting occurs across the U-curves. These figures describe the theoretical basis for chip formation in MAM.

of Fig. 1a decomposes into multiple curves. The U-shaped curve shown in the figure marks the boundary between continuous cutting (i.e., $h(t) > 0$) and discrete cutting where the undeformed chip thickness periodically becomes equal to or less than zero (mathematically $h(t) \leq 0$, but physically $h(t) = 0$). For MAM conditions outside the U-curve (shaded area), the tool is always engaged with the workpiece and cutting is continuous, despite the superimposed modulation. MAM conditions inside the curve (unshaded area) result in discontinuous cutting with discrete chip formation, and disruption of the tool-chip contact in each cycle of modulation. The global minimum or smallest value of A for discrete chip formation is given by $2A = h_o$ and occurs when $\varphi = \pi$; this value of φ corresponds to $f_m/f_w = ½(2N+1)$, where N is an integer. This modulation condition, with $f_m/f_w = ½(2N+1)$ and peak-to-peak amplitude, $2A = h_o$, has been labeled as the optimum modulation condition [12, 13]. At other values of this frequency ratio, the minimum peak-to-peak amplitude, 2A, for discrete chip formation is greater than h_o. Modulation alone may not always be sufficient to realize discrete chips, as seen from Fig. 1. At the asymptotic ends of the U-curves ($f_m/f_w = N$) successive cutting cycles are 'in phase' and discrete chip formation is never realized regardless of magnitude of A. Instead, a continuous chip should be expected to form. Amplitude-frequency conditions for discrete chip formation with tools having multiple cutting edges can be established in an analogous way. For a tool with k cutting edges, the optimum modulation condition becomes $2A = h_o/k$ with $f_m/f_w = k(2N+1)/2$.

The amplitude condition for discrete chip formation and tool-chip contact disruption can be realized in MAM even at high cutting speeds [13, 15], in contrast to the velocity-modulation case. For example, since amplitudes as large as 0.2 mm can be achieved using piezo-type actuators in low-frequency modulation, MAM is capable of effecting discrete chips even at cutting speeds of ~ 1000 m/min. This makes feed-modulation especially well-suited for implementation at speeds typical of industrial practice. The superimposition of the modulation to the machining does not change the MRR which is determined by the baseline machining parameters.

Fig. 1 provides guidelines for setting the amplitude-frequency conditions to effect discrete chip formation. In general, the minimum amplitude (optimum) condition is to be preferred, unless process constraints warrant otherwise. Of course, in practice, the modulation amplitude may have to be set somewhat higher than the minimum values to compensate for system compliance. It may generally be preferable to use the larger values of the f_m/f_w ratio (Fig. 1b), as this would cause the chip formation to be interrupted more frequently, resulting in smaller discrete chips and improved lubrication of the contact. Indeed, large values for this ratio result in very short chips, an aspect exploited in production of particulate and fibers by MAM [16]. However, the largest f_m/f_w ratio achievable in practice will be determined by the maximum amplitude that the modulation device can sustain at a particular frequency. To avoid rubbing between the tool flank and the freshly generated surface, the tool clearance angle has to satisfy a constraint given by $\beta > \tan^{-1}[(h_o f_w + 2\pi f_m A)/(\pi d f_w)]$. This is generally met in practice [17, 18].

Results, Capabilities, Applications

A series of experiments was carried out to verify the theoretical basis of MAM, and demonstrate various capabilities and applications of MAM. The experiments were carried out in single-point turning and drilling configurations. The experiments employed a commercial modulation device (M4 Sciences LLC) that could impose the feed modulation (Fig. 2). This device is compact, easily incorporated into industrial machining systems, and employs a piezo-electric actuator to impose the modulation (amplitudes of up to 0.2 mm and frequencies up to 1000 Hz [15]). Since the modulation is applied locally at the tool, inherent dynamic and inertia effects are minimized; such effects cause complications (e.g., control of amplitude, frequency) when attempting to modulate machine slides with relatively large mass [12, 19]. The commercial system for MAM enables controlled experimental investigation of the process over a range of machining conditions.

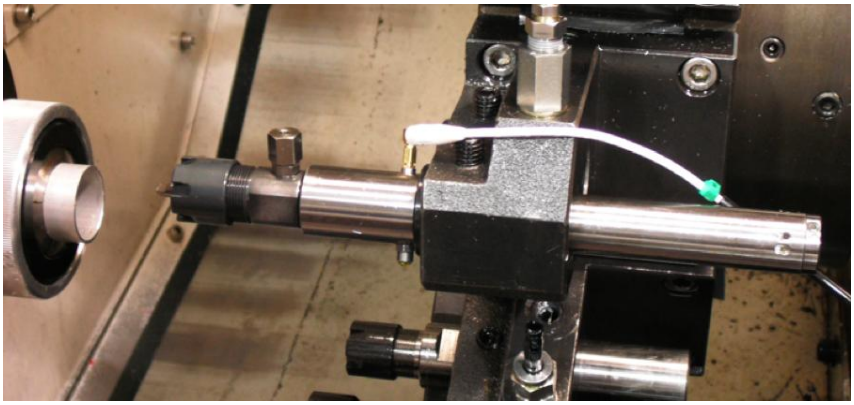

Figure 2 Commercial modulation device used in MAM experiments. The left hand side of the image also shows an aluminum tube workpiece used in some turning experiments.

The results presented in the ensuing cover the following a) verification of theory of discrete chip formation and tool-chip contact disruption in MAM, as demarcated by the cutting regimes of Figure 1, b) case-studies of MAM in drilling under conditions typical of industry practice that demonstrate enhancement of material removal rate (MRR), improved chip management and fluid action, and reduction of tool wear and c) new applications of machining enabled by MAM – fiber production, surface texturing, and chip re-use/recycling.

Discrete Chip Formation. Figure 3 shows pictures of the chips formed when turning Al6061-T6 tube at select MAM conditions, together with the U-curve demarcating the cutting regimes. The chip morphologies confirm the predictions of chip formation in the two MAM regimes. In the discrete cutting regime, the chips are much smaller in size, than in the continuous cutting regime. The transition from continuous to discrete cutting when traversing across the U curve is evident in

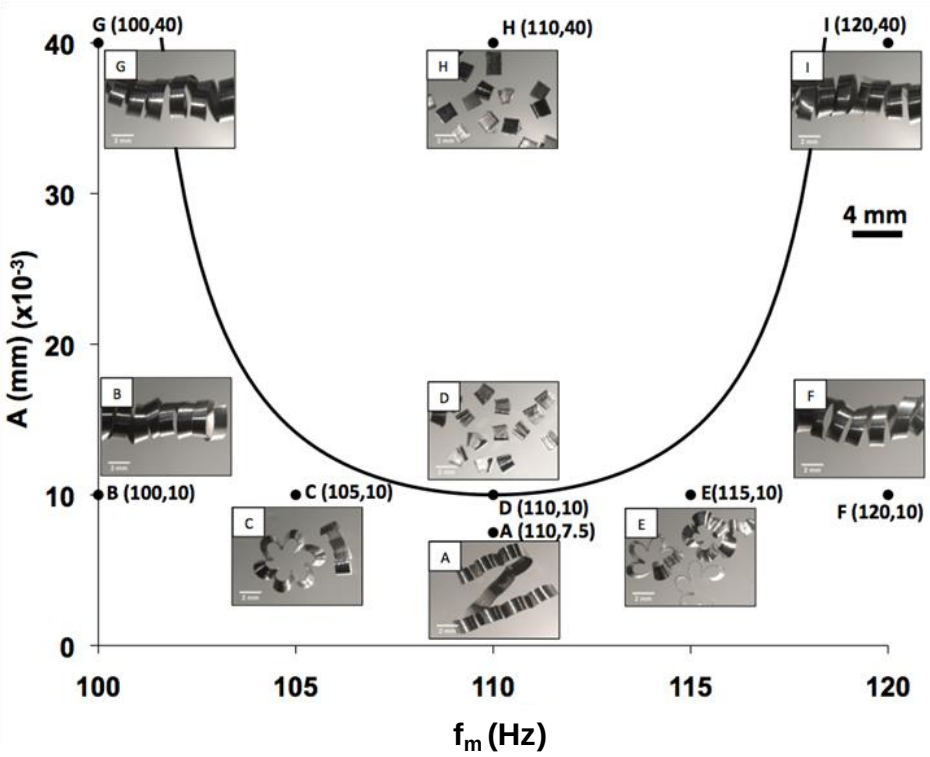

Figure 3 Optical microscope pictures showing chip forms created at the various MAM conditions; machining conditions: f_w = 20 Hz, h_o = 0.01875 mm (feed/rev, machine setting), depth of cut = 1.2 mm, d = 25.4 mm. Note the close correspondence between predicted and observed chip formation at the conditions tested (f_m, A).

the figure. Furthermore, continuous chips are seen to always occur at the asymptotes of the U-curve, irrespective of the modulation amplitude (Fig. 3), indicating that the application of a modulation, even of very large amplitude, is in itself not sufficient to achieve discrete chip formation.

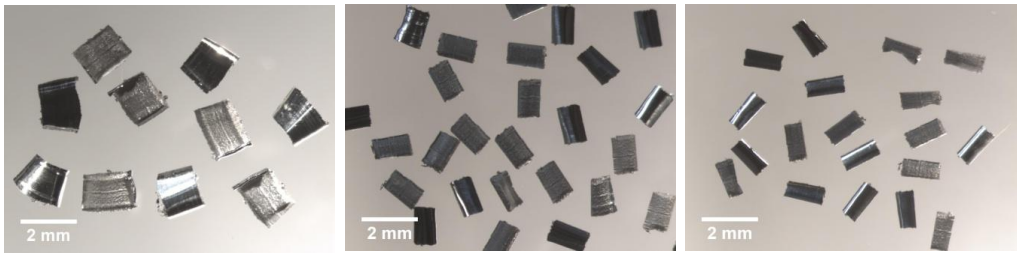

$f_m/f_w = 5.5$
$A = 0.015$ mm

$f_m/f_w = 15.5$
$A = 0.020$ mm

$f_m/f_w = 20.5$
$A = 0.023$ mm

Figure 4 Chips generated at increasing values of the ratio f_m/f_w (f_w = 20 Hz). The top row corresponds to MAM conditions of continuous cutting and the bottom row to discrete cutting. All of the pictures are at the same magnification.

The effect of modulation on chip morphology was also explored by fixing the amplitude at a value sufficient to effect discrete chip formation and varying f_m/f_w. Figure 4 shows some chips obtained from these experiments; as f_m/f_w is increased, the chip lengths become smaller in a manner consistent with discrete chip segments being formed at the rate of f_m/f_w per revolution. These observations are again consistent with predictions of the chip formation model for turning (k = 1). Predictions of chip formation characteristics for tools with multiple cutting edges were likewise verified using drilling (k = 2, 3 (2- and 3-fluted drills)) and end milling (k = 4) experiments. An example of the role of modulation in effecting discrete chip formation with 2-fluted drills is shown in Fig. 5.

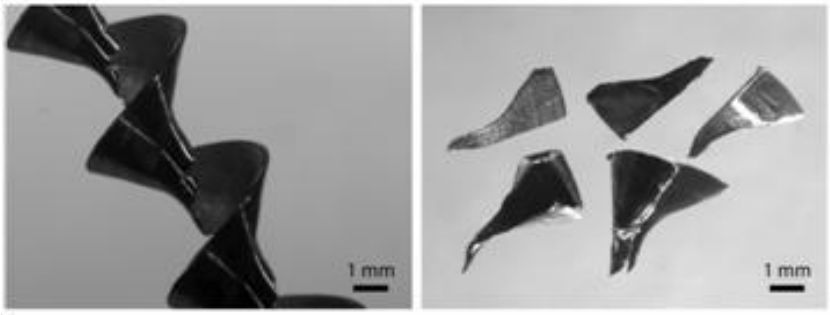

(a) **(b)**

Figure 5 OFHC copper chips generated during two-flute drilling at f_w = 80 Hz, h_o = 0.1 mm/rev, d = 7 mm, with (a) conventional drilling and (b) f_m = 240 Hz, A ~ 0.025 mm.

Drilling Case Studies. A series of drilling tests typical of industrial-application cases was carried out to demonstrate benefits of MAM arising from discrete chip formation and disruption of tool-chip contact. Most of these tests involved drilling with a 2-fluted drill under conditions typical of industry operations wherein process performance is known to be determined by effectiveness of evacuation of chips from the drilling zone deep inside a hole. Process attributes such as material removal rate, cycle time, deep-drilling capability (length-to-diameter (L/D)) and tool wear were used to make the performance assessments. The work materials e.g., stainless steels, Inconel® 718, Hastelloy® 625, for the tests fall in a category that is often considered difficult to machine. The results of some of these tests are presented in Table 1, with the bold face entries representing performance-related outcomes. The extraordinary capability of MAM is evident from the performance improvements seen in the results and the comparison with conventional (baseline) drilling. To note, the principal difference in these tests with MAM was in the use of modulation,

typically at or near an optimum modulation setting, to effect discrete chip formation and contact disruption.

Table 1 Performance attributes of MAM and baseline machining

Test	Attribute	Description	Tooling	Fluid	Workpiece	Baseline Machining Conditions	MAM Conditions
1	Cycle time	Drilling 3.5 mm dia, 105 mm deep hole	Single flute carbide coolant fed gun drill	Oil, 80 bar	Titanium alloy Ti6Al4V	4200 RPM (fw = 70 Hz), 0.015 mm/rev, **105 sec drilling time**	f_m = 105 Hz, $A \approx$ 0.012 mm, 0.020 mm/rev, **75 sec drilling time**
2	Tool Wear	Drilling, 0.32 mm dia, 2.5 mm deep hole	2-flute carbide TiN coated high speed steel cobalt twist drill	Oil, flood	Steel alloy 4140	9660 RPM (fw = 161 Hz), 0.005 mm/rev, **PECK CYCLE 0.150 mm/peck, 8 sec drilling time, drill life ≈ 250 parts**	f_m = 161 Hz $A \approx$ 0.004 mm, **NO PECK CYCLE, 4 sec drilling time, drill life ≈ 600 parts**
3	Drilling beyond flute	Drilling, 0.760 mm dia, 14.50 mm deep hole	2-flute uncoated carbide twist drill, 12.5mm flute length	Oil, flood	Nickel alloy Inconel® 718	4020 RPM (fw = 67 Hz) 0.005 mm/rev, 0.125 mm/peck, 24 sec drilling time, **Drilling beyond flutes caused drill failure**	f_m = 67 Hz, $A \approx$ 0.002 mm, 0.250 mm/peck, 15 sec drilling time, **Drilling 2.5 mm beyond drill flute**
4	Length to Diameter L/D	Drilling 1.2 mm dia, 15 mm deep hole	2-flute carbide twist drill	Oil, flood	Nickel alloy Hastelloy® 625	2040 RPM (fw = 34 Hz), 0.020 mm/rev, **Depth < 2 mm L/D ~ 1.5**	f_m = 102 Hz, $A \approx$ 0.015 mm, **Depth > 10 mm, L/D ~ 6.5**
5	Tool Wear	Cylindrical turning	Single-point CBN	Oil, mist	Compact Graphite Iron	550 m/min, 1500 RPM (fw = 25 Hz), 0.050 mm/rev, 1 mm depth of cut, **Tool life < 3 minutes**	f_m = 112.5 Hz, $A \approx$ 0.030 mm, **Tool life > 20 minutes**

New Enabling Applications. Since functional characteristics (e.g., running in, oil retention, wear) of components are determined at least in part by their surface texture [20], an exploration of surface texturing (3-D topography) by MAM was undertaken. This surface texturing capability is afforded by the additional degrees of freedom in tool motion inherent to MAM. This capability was explored using simulation and some example cases were demonstrated in turning. The simulation was carried out for cylindrical turning with MAM and involved calculation of cylinder surface topography rather than chip geometry [18]. Fig. 6 shows examples of simulated (steady-state) surface texture for a representative patch of the surface in $\varphi - A/h_o$ space for various modulation frequencies; the shapes of the surface features are primarily determined by φ and A/h_o. Some actual surfaces created by MAM are shown in Fig. 7 (top row) with corresponding simulated profiles

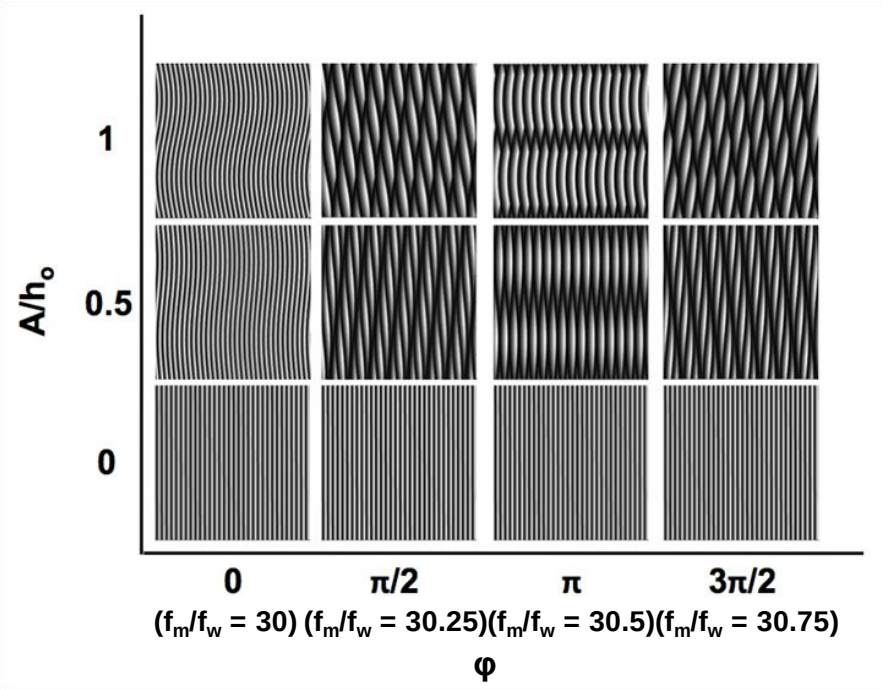

Figure 6 Surface textures over a 0.6 x 0.6 mm2 surface patch as predicted by simulation of MAM. h_o = 0.01875 mm (feed/rev, machine setting), depth of cut = 0.15 mm, tool nose radius ≈ 0.02 mm, rake angle 0 º, lead angle 0 º, front relief angle 5 º.

(bottom row). The correlation between the 2 sets of profiles is quite striking, demonstrating also the capability of the simulation as a tool to explore surface generation in MAM. The types of surface texture shown are quite remarkable and difficult to achieve in practice on metal surfaces over large areas using conventional removal processes [20].

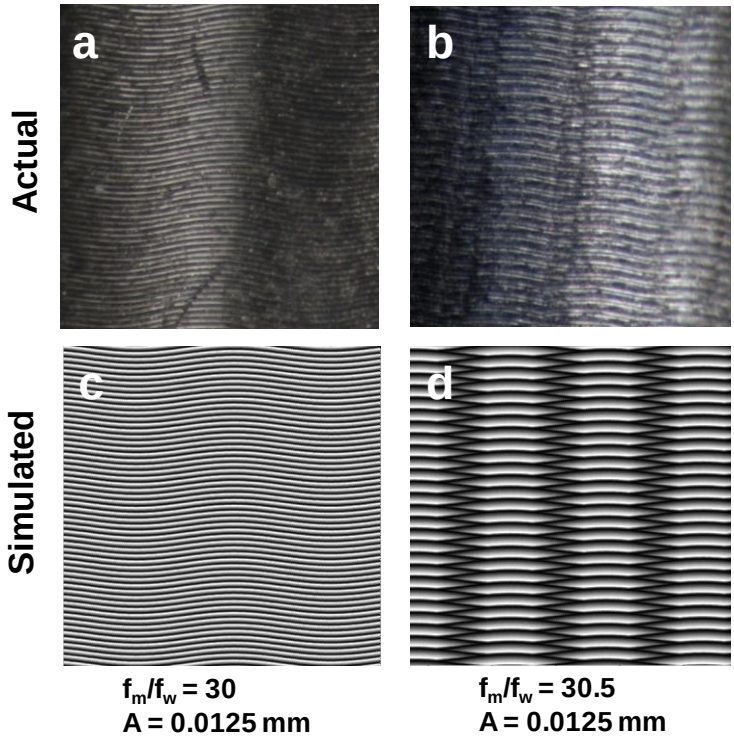

Figure 7 Surface textures created in conventional cylindrical turning and MAM. The images show a 1 x 1 mm^2 surface patch with the actual images being optical microscope pictures of surface patches created in experiments. h_o = 0.01875 mm (feed/rev, machine setting), depth of cut = 0.15 mm, rake angle 0º, lead angle 0º, front relief angle 5º, tool nose radius is ≈ 0.02 mm.

Another application of MAM that is enabled by the controlled discrete chip formation is production of powder particulate (~ 0.020 mm to several mm) with extraordinary size and shape control using chip formation. Figure 8 shows one such example involving production of metal alloy fibers of high-aspect ratio, about 25 micrometers in equivalent diameter and about 6 mm long, from Al6061-T6.

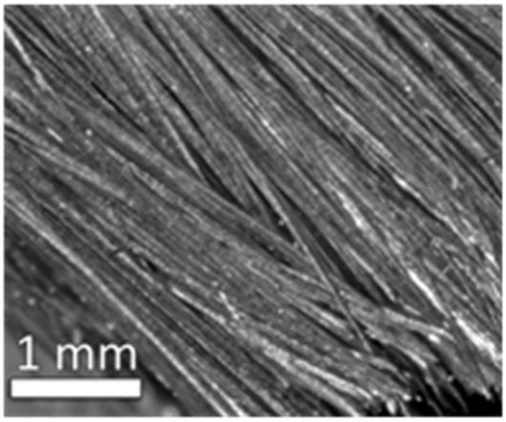

Figure 8 Al6061-T6 fibers produced by MAM (f_m = 1801.5 Hz, A ~ 0.001 mm) using cylindrical turning at f_w = 180 RPM, h_o = 0.002 mm/rev, depth of cut = 6 mm.

These were produced at the rate of ~ 1800/s. Production of particulate with shapes such as platelet and equiaxed is also feasible and has been demonstrated [16-18]. The process is scalable for large-volume production of fiber and particulate from almost any metal or alloy system. In combination with the simulation capability for MAM that has been developed, opportunities exist for developing a class of fiber and powder (materials) manufacturing applications for machining.

A note about recycling/re-use of chips facilitated by MAM is in order before concluding. Chips of small, well-defined size such as created by MAM can be much more efficiently stored, handled and re-processed. 'Small chips' of controlled size are also better suited for consolidation into bulk forms or for use as reinforcements in various matrices enabling opportunities for recycling of chip streams into higher value products. Given the large quantities of chips produced as 'waste streams' in industrial operations worldwide, these aspects of MAM offer additional attractive benefits in terms of improving sustainability of machining processes.

Concluding Remarks

Modulation-assisted machining (MAM) represents a new paradigm in machining technologies in that it employs modulation in a 'constructive way', enabling unprecedented enhancements in productivity, performance and capability of material removal processes. It enables new applications of machining in particulate materials manufacturing and surface texturing. And it advances the contrarian view that 'good vibrations' exist in machining.

Acknowledgement

This work was supported in part by NSF grant CMMI-0928337 to Purdue University; and NSF grants STTR-IIP-0944980 and SBIR-IIP-0822879 to M4 Sciences LLC.

References

[1] M.C. Shaw: *Metal cutting principles* (Oxford Univ. Press, Oxford 1984).

[2] K. Nakayama: Bull. Fac. Eng. Yokohama Natl. Univ. Japan Vol. 8 (1959), p. 1.

[3] E.D. Doyle, J.G. Horne and D. Tabor: Proc. R. Soc. Lond. A. Math. Phys. Sci. Vol. 366 (1979), p. 173.

[4] V. Madhavan, S. Chandrasekar and T.N. Farris: J. Tribol. Vol. 124 (2002), p. 617.

[5] L. De Chiffre: Int. J. Mach. Tool Des. Res. Vol. 17 (1977), p. 225.

[6] C. Huang, S. Lee, J.P. Sullivan and S. Chandrasekar: Tribol. Lett. Vol. 28-1 (2007), p. 39.

[7] S. Tobias and W. Fishwick: Trans ASME Vol. 80 (1958), p. 1079.

[8] S. Doi and S. Kato: Trans ASME Vol. 78 (1956), p. 1127.

[9] H. Findley, US Patent 3,174,404. (1965)

[10] J. Kumabe: *Vibration cutting – basic principle and application* (Jikkyo Shuppan Books, Japan 1979).

[11] W. Moscoso, E. Olgun, W.D. Compton and S. Chandrasekar: J. Tribol. Vol. 127 (2005), p. 238.

[12] P.N. Chhabra, B. Ackroyd, W.D. Compton and S. Chandrasekar: Proc. Inst. Mech. Eng. B: J. Eng. Manuf. Vol. 216 (2002), p. 321.

[13] J.B. Mann, C. Saldana, W. Moscoso, W.D. Compton and S. Chandrasekar: Tribol. Lett. Vol. 35-3 (2009), p. 221.

[14] T. Moriwaki and E. Shamoto: Ann. CIRP Vol. 40-1 (1991), p. 559.

[15] J.B. Mann, S. Chandrasekar and W.D. Compton, US Patent 7,587,965. (2009)

[16] J.B. Mann, C. Saldana, S. Chandrasekar, W.D. Compton and K.P. Trumble: Scr. Mater. Vol. 57-10 (2007), p. 909.

[17] J.B. Mann, S. Chandrasekar and W.D. Compton, US Patent 7,628,099. (2009)

[18] C. Saldana: MS Thesis, Purdue University, US. (2006)

[19] S. Smith, B. Woody, W. Barkman and D. Tursky: Ann. CIRP Vol. 58-1 (2009), p. 97.

[20] K.J. Stout, E.J. Davis and P. Sullivan: *Atlas of machined surfaces* (Chapman and Hall, UK 1990).

Modelling of Machining Operations
10.4028/www.scientific.net/AMR.223

Modulation-Assisted Machining: A New Paradigm in Material Removal Processes
10.4028/www.scientific.net/AMR.223.514